Memoirs of the Faculty of Engineering, Nagoya University
Vol. 43, No.1 (1991) — Research Report —

NUMERICAL STUDY ON THE INTERACTION OF SUPERSONIC FLOW PAST A WEDGE AND FREE JET

Takeo SOGA and Kouji YAMANAKA

Department of Aeronautical Engineering

(Received May 31, 1991)

Abstract

A supersonic flow past a swept or unswept ramp with the free jet ejected from the ramp end is simulated numerically employing the Piecewise Linear Method within the framework of the Euler equation. Results of simulation in the two-dimensional flow configulation predicted that a refected shock wave interacted with the free jet resulting a pressure disturbance in the flow. Results of the simulation for the swept ramp predicted that a spiral flow emerged from the ramp-side involved the free jet resulting in a pair of unified intensive vortices. This vortex stretched the fuel jet crosswise and lifted it up. Such a stretching motion of the vortex effected the increase of the contact surface of the main flow and free jet, i.e., air and fuel. Thus the effectiveness of the swept ramp injector for the mixing enhancement of fuel-air was asserted. Further studies based on the Navier-Stokes equation is necessary, which will reveal whether or not the pair of vortices is stationary.

1. Introduction

Research and development for advanced aerospace propulsion system has been extensively performed in Japan and abroad, especially in the United States. One of the proposed air breathing engines is a hydrogen-fueled supersonic combustion ramjet (scramjet) engine that is capable of propelling a vehicle at hypersonic speed in the atomosphere or beyond the atmosphere into orbit. One of the most important requirements of the scramjet engine is a high efficiency of fuel-air mixing (mixing enhancement) and reactions taking place in the engine. The research has recently been directed toward the development of various models of the scramjet engine with which such a high efficiency is fulfilled.

It is well known that the spreading rate of supersonic mixing layer decrease with increasing Mach number[1]. This decrease is attributed to the stabilization of the supersonic flow[2]. Thus the fuel-air mixing enhancement may be realized in an instabilized flow, in turbulence or in the secondary flow with vorticity induced in the flow. Many experiments revealed that mixing enhancement could be acheived through the interaction of parallel jet and transverse jets[3], through the interaction of shock wave and jets[4], and through the strong shear layer produced in the flow[5].

Researchers at NASA Langley Research Center devised a parallel injector ramp as a model of actual combuster configulation[6]. In this combustor configulation supersonic intake flow past the ramp decelerates slightly through the oblique shock and then it accelerate through the Prandtl-Meyer expansion around the corner of the back step of the ramp. The oblique shock wave reflect at the upper wall of the combustor and this reflected wave interacts with the expansion fan. The reflected wave further reflects at the lower wall of combustor behind the ramp. Fuel (hydrogen) is injected from the end-wall of the ramp into the ineraction zone of shock wave and expansion fan. The reflected shock wave ineracts with the fuel jet, enhancing fuel-air mixing. Swept ramp causes a streamwise vortex as well as a crossweise vortex. These vortices interact with the fuel jet, resulting in pronounced fuel-air enhancement. Such a circulation may be useful to sustain the combustion flame. Experiments of fuel-air mixing and combustion yielded satisfactory results[6].

Numerical simulation of the flow in the abovementioned combustor configulation was also carried out extensively[7], using the three-dimensional Navier-Stokes equation and Baldwin-Lomax turbulence model[8]. A comparison of the results of numerical simulation with the experiment showed an apparent discrepancies, for example, the shock angle of the oblique shock wave and the position of the interaction zone of shock wave and expansion fan. These discrepancies may be attributed to techniques of numerical simulation and will be improved eventually.

Present authors are interested in the abovementioned combustor configulation and want to know the details of the flow field in the combustor. So the authors intend to perform such an improvement themselves, aiming at an accurate prediction of shock waves and expansion waves. Present numerical simulation is directed to grasp the overall structure of the flow field rather than the details of mixing enhancement. Numerical simulation is carried out with in the framework of the Euler equation. Since the Pieceweise Linear Method (PLM)[9] yields good results for the numerical analysis of shock waves and expansion waves, PLM is employed in the present numerical simulation.

2. Numerical Analysis

A. Basic Equation

Flow field of the model combustor with parallel injector ramp is very complex, involving interaction of reflected shock wave with expansion wave and interaction of fuel jet and vortices emerged from ramp side. In order to describe the overall flow field, the three-dimensional Euler equation is employed. The governing equation is written in the conservative form;

$$\frac{\partial U}{\partial t}+\frac{\partial F(U)}{\partial x}+\frac{\partial G(U)}{\partial y}+\frac{\partial H(U)}{\partial z}=0 \tag{1}$$

where

$$\mathrm{U}=\begin{bmatrix}\rho\\ \rho u\\ \rho v\\ \rho w\\ e\end{bmatrix},\quad \mathrm{F}=\begin{bmatrix}\rho u\\ \rho u^2+p\\ \rho uv\\ \rho uw\\ u(e+p)\end{bmatrix},\quad \mathrm{G}=\begin{bmatrix}\rho v\\ \rho uv\\ \rho v^2+p\\ \rho vw\\ v(e+p)\end{bmatrix},\quad \mathrm{H}=\begin{bmatrix}\rho w\\ \rho uw\\ \rho vw\\ \rho w^2+p\\ w(e+p)\end{bmatrix} \tag{2}$$

Notations used in the equation are conventional ones. The ratio of specific heats γ is considered to be constant, $\gamma = 1.4$.

B. Piecewise Linear Method

Godunov's method (see Holt[10]) can be improved, approximating flow properties in the cell by linear functions[11]. This improved method is called as Piecewise Linear Method (PLM), which retains higher order accuracy. Colella and Woodward[12] extended this idea further and proposed Piecewise Parabolic Method (PPM). In Godunov's method unsteasy flow is resolved to the Riemann problems (shock tube problems) of many cells where the boundaries of each cell are regarded as menbranes in the shock tube. Speed up of the Godunov's method was done by Gottlieb and Groth[13] and further by Collera[14] and Collera and Glaz[15] employing approximate Riemann solver. Since the results of PPM[16] showed no remarkable improvement to the PLM, we employ the PLM in the present numerical analysis of the three-dimensional flow.

Introducing the time splitting method proposed by Strang[17], the basic equation (1) can be splitted to three one-dimensional partial difference equations,

$$\frac{\partial \mathrm{U}}{\partial t}+\frac{\partial \mathrm{F}}{\partial x}=0 \tag{3}$$

$$\frac{\partial \mathrm{U}}{\partial t}+\frac{\partial \mathrm{G}}{\partial y}=0 \tag{4}$$

$$\frac{\partial \mathrm{U}}{\partial t}+\frac{\partial \mathrm{H}}{\partial z}=0 \tag{5}$$

If Eqs. (3) to (5) yield

$$\mathrm{U}^{n+1}=S^{x}_{\Delta t}\mathrm{U}^{n} \tag{6}$$

$$\mathrm{U}^{n+1}=S^{y}_{\Delta t}\mathrm{U}^{n} \tag{7}$$

$$\mathrm{U}^{n+1}=S^{z}_{\Delta t}\mathrm{U}^{n}, \tag{8}$$

solution of Eq. (1) can be given by

$$\mathrm{U}^{n+1}=S_{\Delta t}\mathrm{U}^{n},$$

where U^n and U^{n+1} are respectively the solution of Eq. (1) at $t = t^{n+1}$ $(= t^n + \Delta t)$. The difference operator $S_{\Delta t}$ can be expressed as

$$S_{\Delta t} = S^x_{\frac{\Delta t}{2}} S^y_{\frac{\Delta t}{2}} S^z_{\Delta t} S^y_{\frac{\Delta t}{2}} S^x_{\frac{\Delta t}{2}} \tag{9}$$

where the operator $S_{\Delta t}$ retains the second order accuracy.

Employing the time splitting method, the three-dimensional problem is thus reduced to the one-dimensional problems. The numerical simulation proceeds through the following five steps; we assume that we know all U^n:

1. Obtain the distributions of p, ρ, and u in the cell of simulation.

2. Obtain the value of p, ρ, and u at the boundaries (right and left) of the cell at $\Delta t/2$.

3. Solve the Riemann problem, employing the p, ρ, and u at the both side of the boundary (this boundary is equivalent to the membrane of shock tube) as the initial conditions and obtain the values of p, ρ, and u after breakdown of the membrane.

4. Evaluate $F^{t+\Delta t/2}$ at the boundary.

5. Obtain $U_c^{t+\Delta t}$, using the difference equation

$$U_c^{t+\Delta t} = U_c^t + \frac{\Delta t}{\Delta x_j}(F_b l - F_b r)$$

where the subscript r and l denote the right and left boundaries, respectively.

For the sake of time saving Riemann problem is solved employing the Rankine-Hugoniot relation solely[18]. Details of the numerical procedure are shown in references 9. The PLM method was applied to the one-dimensional shock tube problem and the accuracy and the tractability of the method were asserted.

C. *Items of numerical simulation*

Two dimensional flow:

It is very important to know how fuel-jet interacts with the reflected shock wave and the expansion fan around the ramp end. Since in the two-dimensional configulation fine numerical meshs are available, reflection point of oblique shock wave and the abovementioned interaction zone can be predicted unambiguously. So numerical simulation of two-dimensional flow configulation (see Fig. 1) is performed as the first step. Initial conditions and fuel/air flow rate are taken from the experimental condition at the NASA Langley Research Center[6]. We consider the two-dimensional flow field where parallel injector ramps are equiped upper and lower walls of the two-dimensional duct. The flow field below the plane of symmetry is the domain of simulation. Dimensional sizes of the ramp and flow field are as follows: streamwise length is 14 cm, hight of the flow field is 3.9 cm, length of the ramp is 7 cm, hight of the ramp is 1.3 cm, and the wedge angle of the ramp is 10.3 degree. Two uniform flow conditions are chosen: Mach number, velocity, temperature and pressure are respectively M = 2.0, u = 1950 m/sec, T = 1023 K, and p = 10.2 kPa and M = 3.0, u = 1950 m/sec, T = 1023 K, and 10.2 kPa. Fuel is injected parallel to the ramp; M = 1.7, u = 1747 m/sec, v = 308 m/sec, and p = 32.52 kPa. The width of the nozzle of fuel jet is set so that air/fuel mass

flux ratio may yield stoichiometric $H_2 - O_2$ ratio. The boundary conditions of the upstream boundary located a little (0.4 cm) upstream of the leading edge of ramp are given by inflow conditions. The boundary conditions of the downstream boundary are given by the outflow conditions. The boundary conditions of solid walls as well as the surface of symmetry are given by slip conditions except for the fuel jet exit.

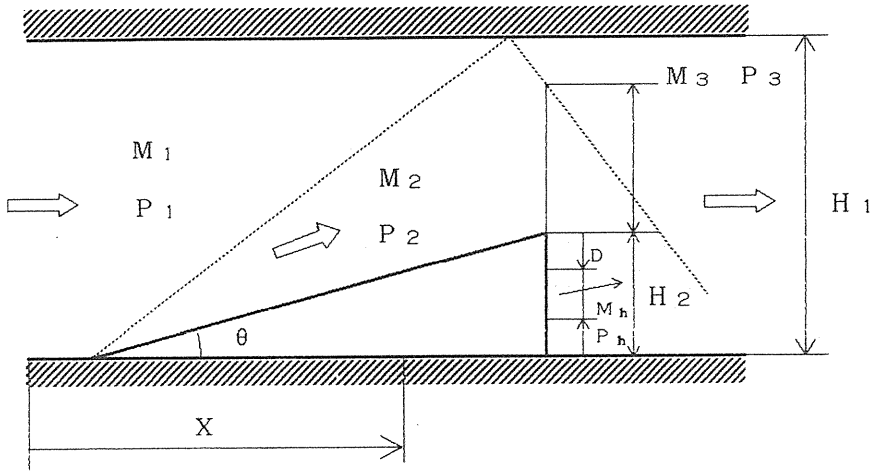

Fig. 1 Schematic drawing of two-dimensional injector ramp.

Three-dimensional flow:

Although fundamental phenomena taken place in the interaction zone can be revealed through the two-dimensional analysis, the flow past the swept ramp is substantially three-dimensional. The interaction of fuel-jet with the spiral flow emerged from the ramp-side may be also essential to the mixing enhancement. In order to perform the three-dimensional analysis the scheme of PLM is extended to three-dimensional one. Such an extension is formally possible employing the time splitting method[17], while we must employ coarse cells in the simulation due to the restrictions on the memory storage and the simulation time. Such a coarse cells may yield less unambiguous shock waves and expansion waves. Numerical simulations are carried out for the swept (see Fig. 2a) and unswept (see Fig. 2b) ramps. The domain of simulation is shown in Figs. 2a and 2b, where the X-Y cross section at $Z = 0$ cm means the surface of symmetry of one ramp and the X-Y cross section at $Z = 2.2$ cm means the surface of symmetry of two ramps. The width of the swept ramp at the leading edge is 2.2 cm and the swept angle is 80 degrees. The width of the ramp-end is 0.8 cm, which is same as the width of the unswept ramp. Initial conditions and boundary conditions are same as the one of the two-dimensional analysis, while the radius of the injector is 0.7 cm. The cell number in the X, Y, and Z directions are 40, 60, and 34, respectively.

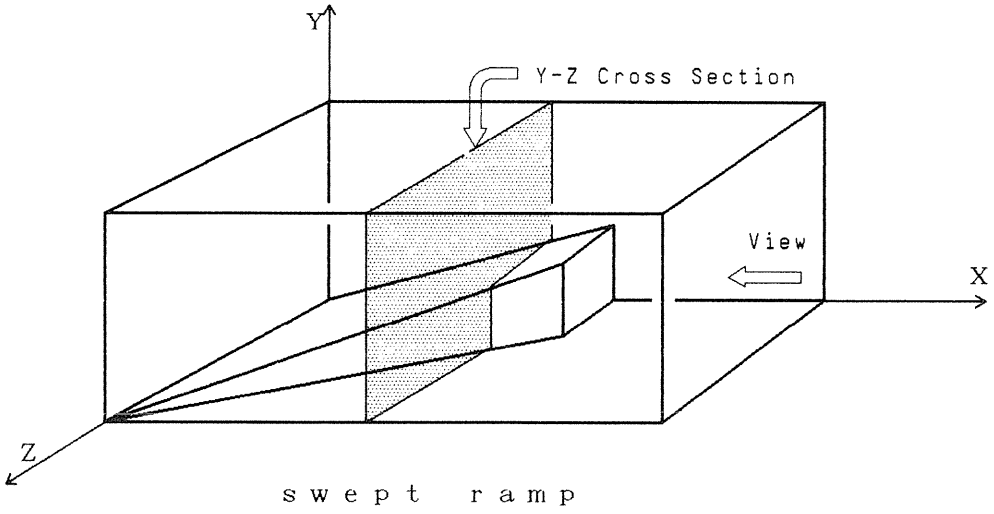

Fig. 2a The domain of simulation (swept ramp); the presented domain is one-eighth of the whole flow field.

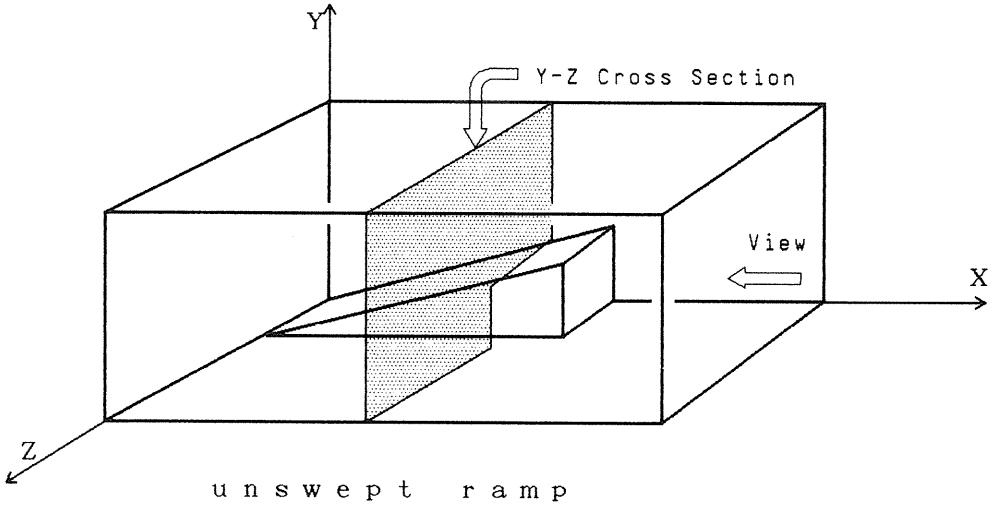

Fig. 2b The domain of simulation (unswept ramp); the presented domain is one-eighth of the whole flow field.

3. Results and Discussion

A. *Results of two-dimensional flow*

Results of numerical simulation are shown in Figs. 3 − 5 for the case of $M_1 = 2.0$. In Figs. 3a and 3b are shown the pressure and density conrours, respectively. Stream lines are shown in Fig. 3c. The numerical results of PLM yield the sharp oblique shock wave, which has the shock angle of 39° corresponding to the theoretical value for $M_1 = 2.0$ and $\theta = 10.3°$ The reflection point of the oblique shock wave (about 5.0 cm downstream from the upstream boundary) agrees well with the experimental results of Northern et al. (see Fig. 9 in Ref. 6).

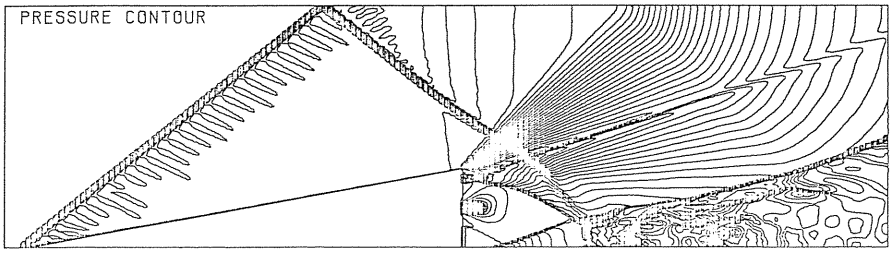

Fig. 3a Pressure contour; $\Delta p = 700 Pa$

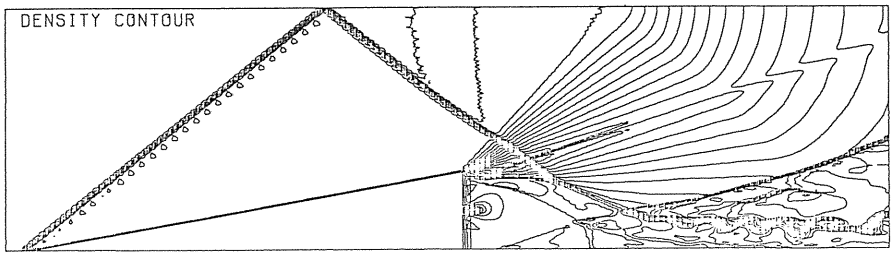

Fig. 3b Density contour; $\Delta \rho = 1.5 \times 10^{-3}\ kg/m^3$

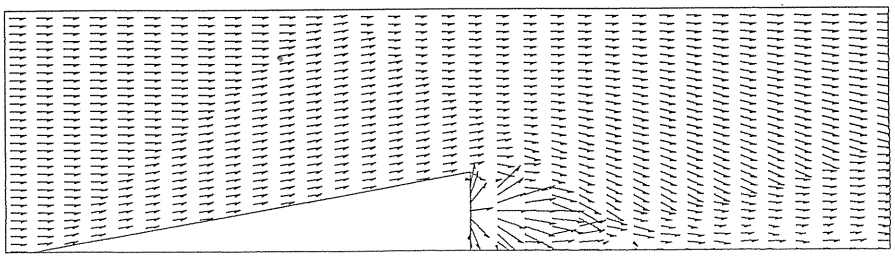

Fig. 3c Stream lines expressed by volocity vectors.

As shown in Fig. 3c the intake flow is passing through the oblique and the reflected shock waves without noticeable deceleration. The reflected shock wave is passing through the expansion wave around the corner of the ramp and interacts with the fuel jet. The jet plume of fuel collides with the lower wall and reflects upperward.

The flow field in the vicinity of the fuel jet is shown in Fig. 4, which is an enlargement of Fig. 3b. The stream lines (Fig. 3c) are folded in the figure. In this figure the contact surface of the main flow and the fuel jet is depected (indicated by the arrow). In Figs. 5a pressure and density along the upper wall are shown. We can find the positions of shock wave and expansion wave from this figure; they are about 5.0 cm and 9.8 cm from the upstream boundary, respectively. Figure 5b shows pressure and density along the lower wall (behind the ramp).

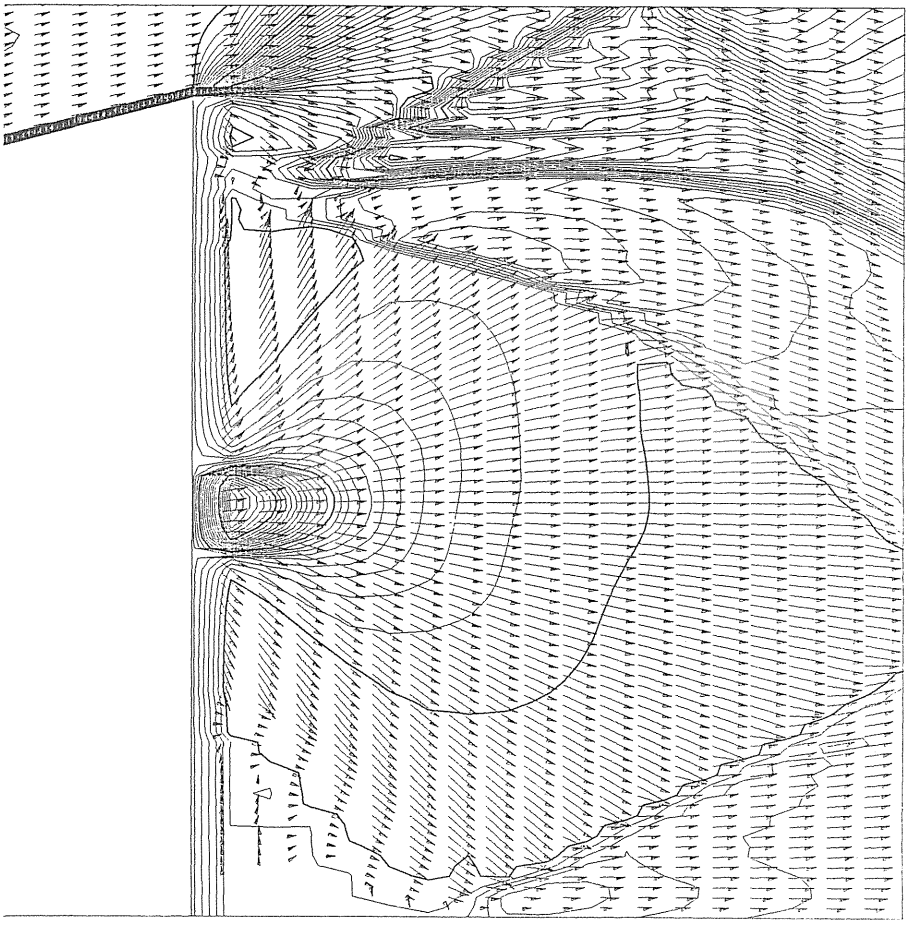

Fig. 4 Density contour and stream lines in the vicinity of the exit of fuel jet; the arrow indicates the contact surface of air and fuel; $\Delta\rho = 1.2 \times 10^{-3}\ kg/m^3$

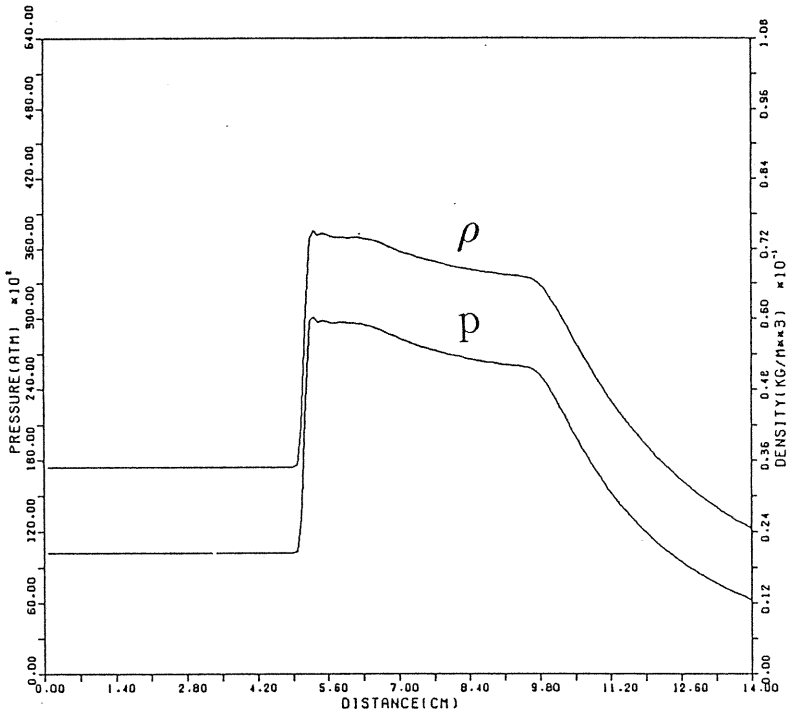

Fig. 5a Pressure and density distributions on the upper boundary of the domain of simulation.

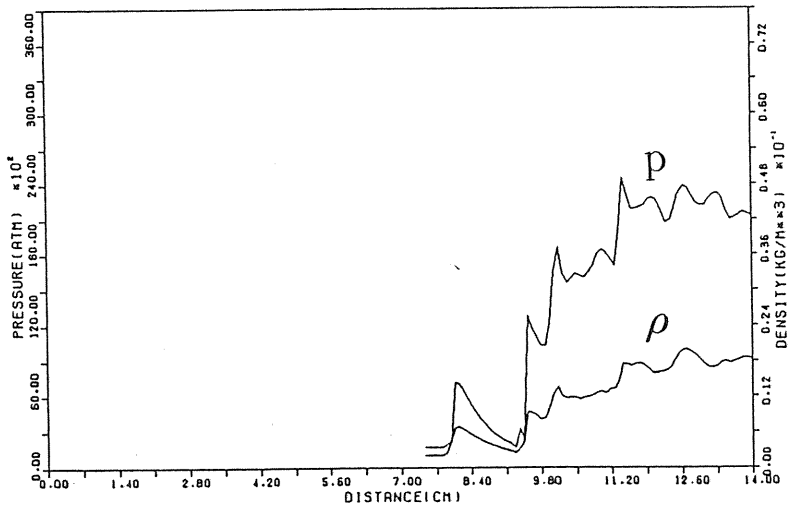

Fig. 5b Pressure and density distribution on the lower wall behind the fuel injector.

Fluctuation in the pressure along the lower wall takes place after the reflected (oblique) shock wave reaches the reflected jet plume (see Fig. 3a); Since the present analysis is based on the Euler equation, discussion on this point should be restriced to a qualitative one. The two-dimensional analysis predicts that the oblique shock wave emerges and reflects as expected and the interaction of shock wave with the fuel jet induces pressure (or density) fluctuation.

Numerical simulation for $M_1 = 3.0$ yielded similar results as the case $M_1 = 2.0$. But the shock angle was 28° and the reflected oblique shock wave reached in the vicinity of downstream boundary of computational domain. No significant interaction was predicted for the present ramp with the wedge angle $\theta = 10.3°$ which was design for $M_1 = 2.0$.

B. Results of three-dimensional flow

Pressure and density contours and stream lines on the streamwise plane (X-Y plane) were similar to the results shown in Fig. 3. Features of the three-dimensional flow, such as spiral flows, can be well expressed on the y-z plane perpendicular to the main flow (see Fig. 2). The direction of view is shown in Fig. 2. Stream lines on the Y-Z plane are presented in Fig. 6 where 6a, 6b, 6c and 6d are corresponding to $X = 2.8$ cm, 7.0 cm, 8.4 cm and 11.2 cm, respectively; the ramp-end is located at $X = 7.4$ cm. Results of the swept and unswept ramps are paralleled in the figures.

Fig. 6a: $X = 2.8$ is located slightly downstream from the leading edge of the ramp. Flow along the ramp is expanding at the corner of the ramp side and is accelerated crosswise, forming a vortex perpendicular to the main flow. The combination of the main flow with this vortex results in a spiral flow along the side-wall of the ramp. The vortex emerged from the flow passing through swept ramp is obviously more intensive than the vortex from the flow passing through the unswept ramp. Fig. 6b: $X = 7.00$ cm is located slightly upstream of the ramp-end. The vortex along the swept ramp grows up, involving the most part of the fluid between the ramps and inducing the cross flow on the ramp.

On the other hand the vortex along the unswept ramp is localized at the corner of the ramp-side. Fig. 6c: $X = 8.40$ cm is just downstream of the fuel injector. The vortex along the swept ramp grows up further; the upper part of the vortex interacts with the jet plume extending fuel jet outward, while the lower part of the vortex is gliding beneath the jet plume. Similar vortex motion is seen for unswept ramp but the size of the vortex is much less than the case of swept ramp. Fig. 6d: $X = 11.20$ cm is located slightly downstream of the interaction zone of reflected shock wave with the reflected barrel shock. Here the vortex is involving the fuel jet and results in a unified vortex. This unified vortex effects the mixing enhancement. For the case of unswept ramp two localized vortexes emerge and less efficient mixing enhancement of fuel and air is predicted.

Since the intake flow (air flow) and the fuel jet have the different stagnation pressures, contact surface of the air flow and the fuel flow can be predicted tracing the density contours (see Fig. 4). Figure 7a shows the density contour just behind the fuel injector. A steep change in density around the ramp-end may be caused by the vortex motion (see Fig. 6c). The core of the fuel jet, i.e., the barrel shock is not as jet involved in the vortex. As shown in Fig. 7b, the fuel jet is eventually involved in the vortex. The vortex finally lifts up the fuel jet upperward. The barrel shock is merged into the vortex. So the concentrated iso-density curves indicates the contact surface. The vortex effects the mixing enhancement streching the fuel jet crosswise and lifting up in the main flow. For the case of the unswept ramp such a extension of the contact surface is more deficient. Roughly speaking the contact surface of the swept ramp is 1.5 times of the contact surface of the unswept ramp.

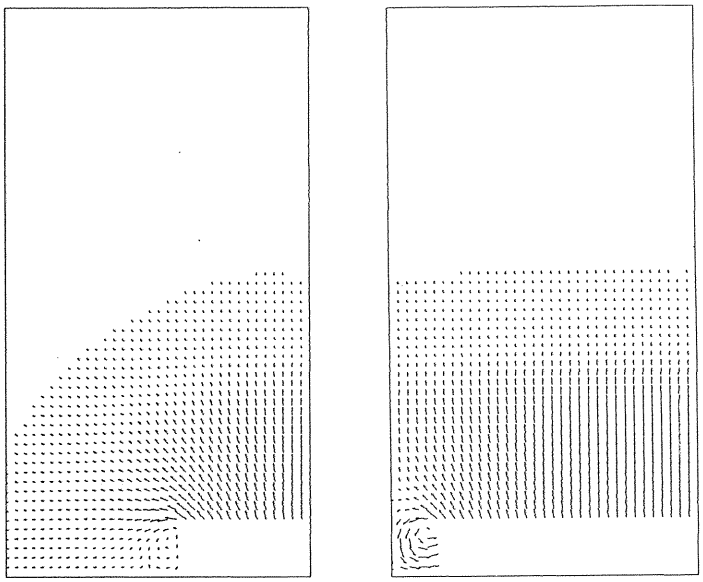

Fig. 6a Stream lines on the Y-Z plane expressed by volocity vectors; X = 2.8 cm.

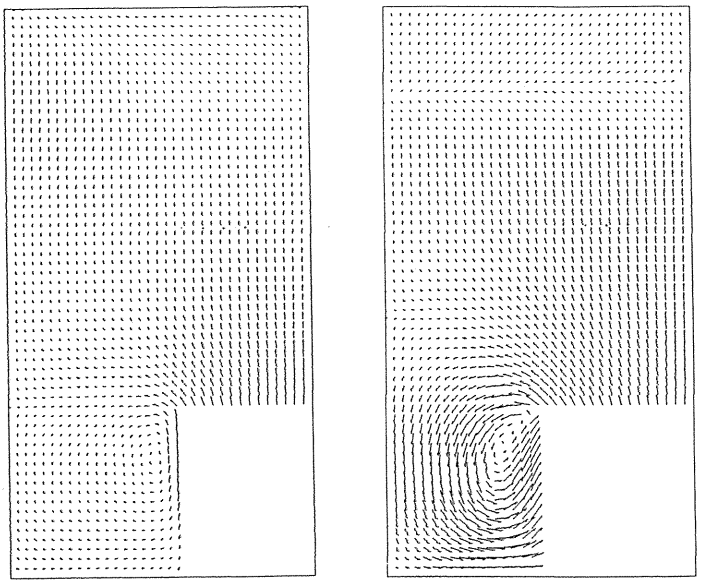

Fig. 6b Stream lines on the Y-Z plane expressed by volocity vectors; X = 7.0 cm.

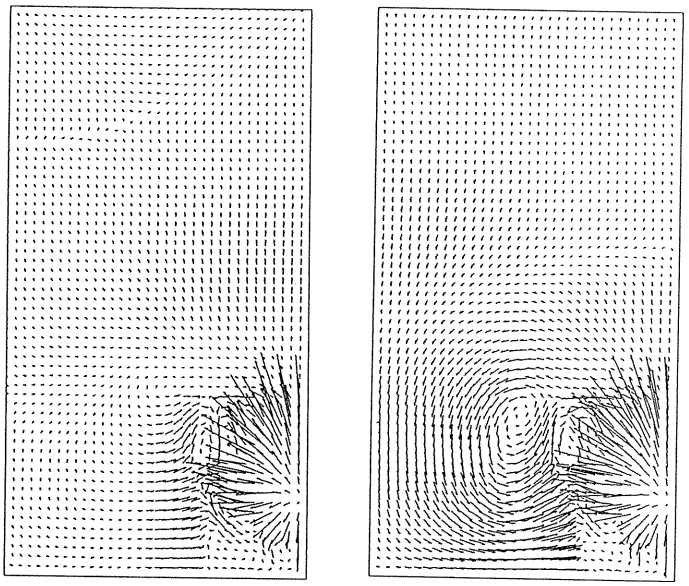

unswept ramp swept ramp

Fig. 6c Stream lines on the Y-Z plane expressed by volocity vectors; X = 8.4 cm.

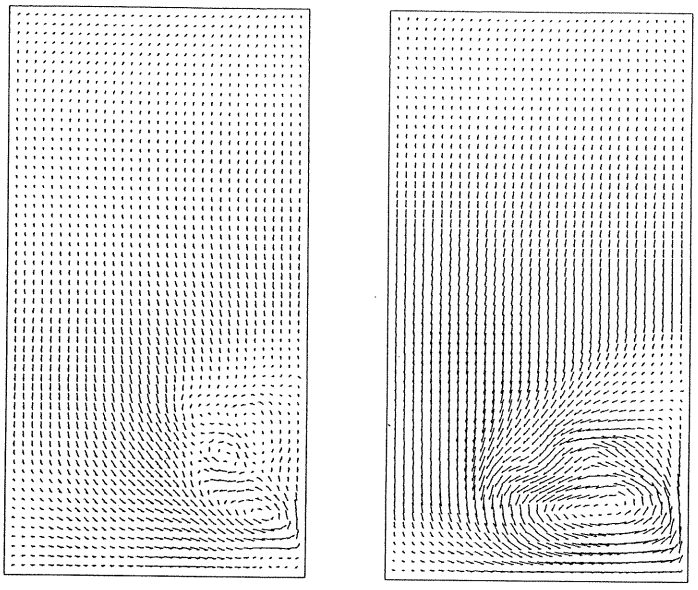

unswept ramp swept ramp

Fig. 6c Stream lines on the Y-Z plane expressed by volocity vectors; X = 11.2 cm.

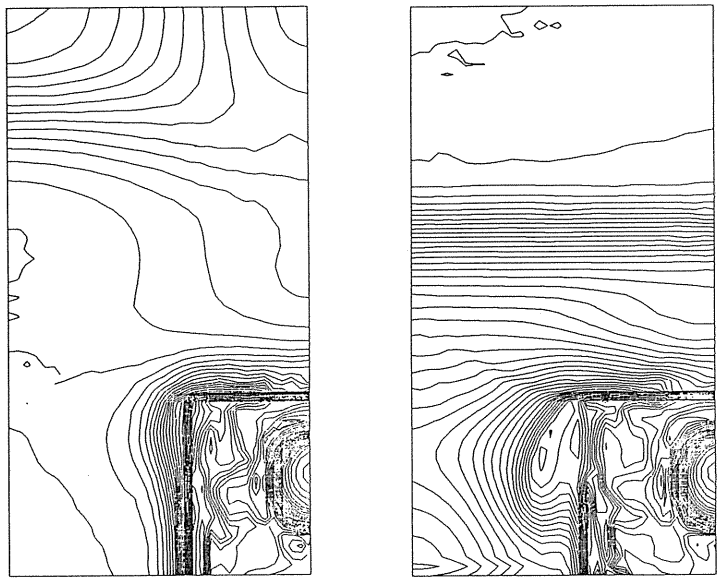

unswept ramp swept ramp

Fig. 7a Density contour on the Y-Z plane; X = 8.05 cm, $\Delta\rho = 1.0 \times 10^{-2}\ kg/m^3$.

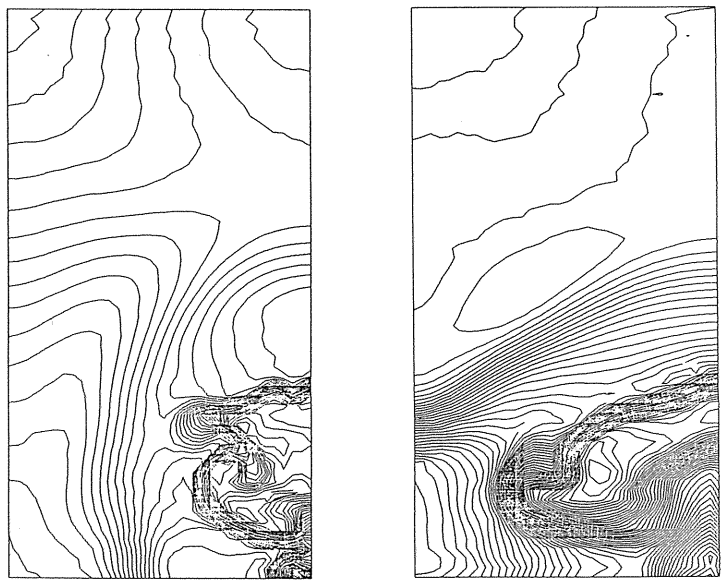

unswept ramp swept ramp

Fig. 7b Density contour on the Y-Z plane; X = 12.25 cm, $\Delta\rho = 1.0 \times 10^{-2}\ kg/m^3$.

Since the X-Y plane at $Z = 0$ is regarded as the surface of symmetry in the present simulation, two symmetric vortices emerge in the flow. But these vortices may be unstable like the Karmann vortices. Such a phenomenon can be simulated employing Navier-Stokes equation. Moreover the formation of the vortex along the ramp-side may be attributed to the virtual viscosity inherent to the numerical simulation. Such a sizable vortex, however, may be expected to take place in the actual flows.

References

1) G. L. Brown and A. Roshko: On the density effects and large structure in turbulence, J. Fluid Mech., Vol. 64, No. 4, pp. 775-816.
2) D. Papamonschou and A. Roshko: Observations of supersonic free shear layers, AIAA Paper 86-0162 (1986).
3) P. S. King, R. H. Thomas, and J. A. Schetz: Combined tangential-normal injection into a supersonic flow, AIAA Paper 89-0622 (1989).
4) S. Menson: Shock-wave-induced mixing enhancement in Scramjet combustion, AIAA Paper 89-0104 (1989).
5) G. A. Sullins, S. A. Luts, D. A. Carpenter, and M. A. Taylor: Experimental investigation of a shear layer in supersonic flow, 1989 JANNAF Propulsion meeting, Cleveland, OH, May 1989. (Cited in Ref. 6).
6) G. B. Northam, I. G. and C. S. Byington: Evaluation of Parallel Injector Configurations for Supersonic Combustion, AIAA Paper 89-2525 (1989).
7) J. P. Drummond, M. H. Carpenter, D. W. Riggins and M. S. Addams: Mixing Enhancement in a Supersonic Combustor, AIAA Paper 89-2794 (1989).
8) B. S. Baldwin and H. Lomax: Thin layer approximation and algebraicc model for separated turbulence flow simulation, AIAA Paper 78-257 (1978).
9) K. Teshima and K. Abe: Analysis of axisymmetric flow employing PLM, Rep. Computer Center of Kyoto Univ., Vol. 19, No.3 (1986).
10) M. Holt: *"Numerical Methods in Fluid Dynamics"*, (Springer-Verlag, 1984) p.28.
11) B. van Leer: Towards the Ultimate Conservative Difference Scheme V. A. Second-Order Sequel to Godunov's Method, J. Comput. Phys., Vol. 32, pp. 101-136 (1979).
12) P. Colella and P. R. Woodward: The Piecewise Parabolic Method (PPM) for Gas-Dynamical Simulations, J. Comput. Phys., Vol. 54, pp. 174-201 (1984).
13) J. J. Gottlieb and C. P. T. Groth: Assessment of Riemann Solvers for Un steady One-Dimensional Inviscid Flows of Perfect Gases, J. Comput. Phys., Vol. 78, pp. 437-458 (1988).
14) P. Colella: A Direct Eulerian MUSCL Scheme for Gas Dynamics, SIAM J. Sci. Stat. Comput., Vol. 6, pp. 104-117 (1985).
15) P. Colella and H. M. Glaz: Efficient Solution Algorithms for the Riemann Problem for Real Gases, J. Comput. Phys., Vol. 59, pp. 264-289 (1985).
16) Y. Kato: Studies on free jets and analysis of high speed flow employing parabolic equation, Master thesis, Dep. Aeronaut. Engng., Nagoya University, 1989.
17) W. G. Strang: On the Construction and Comparison of Difference Schemes, SIAM J. Numer. Anal., Vol. 5, pp. 506-517 (1968)
18) P. Colella: Glimm's Method for Gas Dynamics, SIAM J. Sci. Stat. Comput., Vol. 3, pp. 76-110 (1982).